Computers, Environment and Urban Systems 76 (2019) 1–10

Contents lists available at ScienceDirect

Computers, Environment and Urban Systems

journal homepage: www.elsevier.com/locate/ceus

Automatic cost-effective method for land cover classification (ALCC)

Mateo Gašparović[a,*], Mladen Zrinjski[b], Marina Gudelj[b]

[a] University of Zagreb, Faculty of Geodesy, Chair of Photogrammetry and Remote Sensing, Kačićeva 26, 10000 Zagreb, Croatia
[b] University of Zagreb, Faculty of Geodesy, Chair of Instrumental Techniques, Kačićeva 26, 10000 Zagreb, Croatia

ARTICLE INFO

Keywords:
Landsat-8
Unsupervised classification
k-means
Spectral indices

ABSTRACT

The need for the detection and monitoring of changes in the environment is greater today than ever before. Through classification we can obtain insights into the state of the land surface. No known classification methods are fully automated, and their implementation requires preprocessing and postprocessing. This research provides a novel, fully automatic and cost-effective land cover classification method (ALCC). This novel automatic method does not require prior knowledge of the terrain or the assignment of training samples. The ALCC method is based on unsupervised classification methods, which is performed over the spectral indices rasters and six Landsat-8 30 m spatial resolution bands. The method was tested in three different study areas. Furthermore, all three study areas were classified by common supervised classification methods, namely, the Maximum Likelihood Classification (MLC) and the Random Forests (RF) method. For comparison accuracy, assessment of the three applied classification methods, namely, the figure of merit, overall agreement, omission and commission, were used. The results show that the overall agreement of the new automatic classification method for the Rijeka, Zagreb and Sarajevo study areas is 90.0%, 89.5% and 89.9%, respectively, and the overall agreement always falls between the overall agreement of the MLC method (88.1%, 88.9% and 86.7%, respectively) and the overall agreement of the RF method of classification (91.7%, 90.4% and 90.2%, respectively). These results confirm that this new automatic, cost-effective and accurate land cover classification method can be easily applied for numerous remote sensing applications.

1. Introduction

Currently, many orbiting optical sensors collect land surface data at high spatial and temporal resolutions (Landsat-8, Sentinel-2, RapidEye, PlanetScope, etc.). The main purpose of such satellites is to monitor and detect changes in the Earth's land cover (Clark, Aide, & Riner, 2012; Roy et al., 2014). One of the ways of detecting land cover changes is through the classification of satellite imagery (Xian & Homer, 2010). Change detection can be accomplished using a time series of land cover classifications (Hermosilla, Wulder, White, Coops, & Hobart, 2015).

Land cover classification (LCC) methods for satellite imagery have been developed and tested in various remote sensing studies (Foody, 2002; Gašparović & Jogun, 2018; Gislason, Benediktsson, & Sveinsson, 2006; Otukei & Blaschke, 2010; Pal & Mather, 2003). There are two basic approaches to classification of remotely sensed imagery, namely, supervised and unsupervised (Mather & Tso, 2016). Supervised methods for LCC require prior knowledge of the terrain, as well as training samples to classify the satellite imagery. Many researchers have developed and studied a supervised method for LCC, such as the Maximum Likelihood Classifier (MLC) (Otukei & Blaschke, 2010), Random Forests (RF) (Breiman, 2001) and Support Vector Machine (SVM) (Suykens & Vandewalle, 1999) methods. The basic deficiency of such methods is the need for operator intervention, which slows the processing chain. Unsupervised classification methods are much faster and easier to process and do not require prior knowledge of the terrain and training samples assignment. These methods only require the number of classes involved and the algorithm then classifies the entire scene according to the radiometric characteristics of the pixels. The drawback is that the user must identify real land cover classes based on an unsupervised calculation of these classes. There is a high probability for mixed classes and for other problems. Frequently used methods for unsupervised LCC in use today are k-means (Hartigan & Wong, 1979) and ISODATA (Bezdek, 1980). Recently developed LCC methods are based on machine and deep learning (LeCun, Bengio, & Hinton, 2015; Nasrabadi, 2007), e.g., Neural Networks (Krizhevsky, Sutskever, & Hinton, 2012) and TensorFlow (Abadi et al., 2016). In such methods, it is also necessary to provide a certain number of known training samples for the learning algorithm process. Using the training algorithm, LCC can be applied to similar imagery.

In remote sensing, for fast and accurate detection, monitoring and

* Corresponding author.
E-mail addresses: mgasparovic@geof.hr (M. Gašparović), mzrinski@geof.hr (M. Zrinjski), mgudelj1@geof.hr (M. Gudelj).

https://doi.org/10.1016/j.compenvurbsys.2019.03.001
Received 3 December 2018; Received in revised form 2 March 2019; Accepted 3 March 2019

classification of various land cover classes, various spectral indices have been proposed (Estoque & Murayama, 2015). Spectral indices can also be used to emphasize areas where certain classes are dominant. The normalized difference vegetation index (NDVI) (Tucker, 1979) and soil-adjusted vegetation index (SAVI) (Huete, 1988) emphasize vegetation over other types of land, while the normalized difference water index (NDWI) (Gao, 1996) and modified NDWI (MNDWI) (Xu, 2006) highlight water and the normalized difference bare land index (NBLI) (Li et al., 2017) and normalized difference bareness index (NDBaI) (Zhao & Chen, 2005) indicate bare land.

Influenced by the advantages and disadvantages of the LCC methods mentioned above, this research aims to develop a method for automatic, fast and accurate LCC of satellite images. This newly developed method, ALCC (Automatic Cost-effective Method for Land Cover Classification), is automatic and eliminates the need for training samples or for field knowledge. Furthermore, this method is based on unsupervised classification methods supported by certain types of spectral indices. Similar approaches have thus far been described by some authors (Baraldi, 2011; Baraldi & Boschetti, 2012; Baraldi, Bruzzone, & Blonda, 2005; Baraldi, Puzzolo, Blonda, Bruzzone, & Tarantino, 2006; Li, Wang, Zhong, Zhang, & Liu, 2017). The present method is fully developed, based on open-source software and is applicable to a large number of different types of research. Fast and automatic access to satellite imagery classification allows researchers to create large amounts of spatial data for detection and monitoring changes of the terrestrial surface.

2. Study area and data

For this research, three different study areas covering highly diverse landscapes were selected (Fig. 1). Each study area contained water, vegetation, bare land and urban areas. The first study area covered the area surrounded the city of Rijeka, in the Republic of Croatia and represented a Mediterranean landscape. The second study area covered the region around the capital of Croatia, Zagreb. The third study area was in central Bosnia and Herzegovina and focused on the capital, Sarajevo. The Zagreb and Sarajevo study areas were similar and

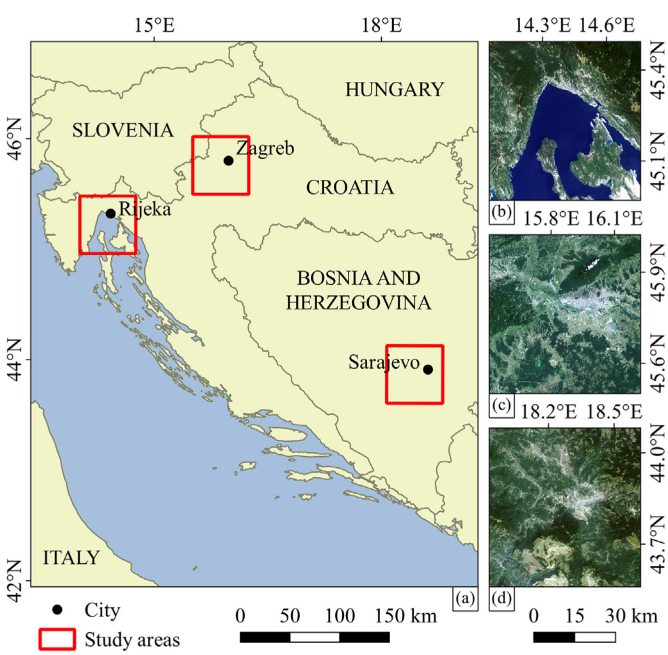

Fig. 1. a) Geographic location of the study areas; b) satellite image of the Rijeka study area; c) satellite image of the Zagreb study area; d) satellite image of the Sarajevo study area. All satellite images use the Landsat-8 "true colour" composite (4–3–2).

represent a continental landscape; however, relief was uniform in the Zagreb study area while the Sarajevo study area was dominated by vegetation and mountains. Each study area had the same dimensions (57 km × 56 km).

Satellite imagery used for this research consisted of cloud-free Landsat-8 imagery (Table 1), obtained during the summer (July or August). Landsat-8 satellite imagery was downloaded from the USGS Earth Explorer service (Roy et al., 2014; https://earthexplorer.usgs.gov/).

The Landsat-8 satellite payload consists of two scientific instruments: The Operational Land Imager (OLI) and the Thermal Infrared Sensor (TIRS). These two sensors provide seasonal coverage of the global landmass at a spatial resolution of 30 m for the visible, near-infrared, and shortwave infrared bands, 100 m for the thermal band, and 15 m for the panchromatic band. The Landsat-8 scene size is 185 km × 180 km (Roy et al., 2014).

3. Methods

A novel method for automatic land cover classification (ALCC) using Landsat satellite imagery was developed in this research. The method is based on a combination of spectral indices and k-means unsupervised classification. For clarity, the new automatic land cover classification method described in this section is divided into three main steps described in the following subsections. Furthermore, the classification accuracy assessment methodology is presented.

3.1. Preprocessing

The atmosphere exerts an influence on radiation signals recorded by satellite sensors through scattering, absorbing and refracting light; therefore, when the land surface reflectance is measured, an atmospheric correction must be performed to correct for atmospheric effects on satellite scenes (Zhang, He, & Wang, 2010). The Dark Object Subtraction 1 (DOS1) atmospheric correction assumes that the atmospheric transmittance in the illumination direction and in the viewing direction are in unison and that the diffuse downwelling irradiance is zero (Chavez, 1989). This method has been found to be data dependent and is well accepted by the geospatial community for correcting light scattering in remote sensing data (Song, Woodcock, Seto, Lenney, & Macomber, 2001). The DOS1 atmospheric correction was performed in the QGIS software (version 2.18.19). The brightness temperature for conversion to degrees Celsius was made for Landsat-8 band 10 (Thermal Infrared band, TIR) during preprocessing in the QGIS software. Observed band 10 thermal radiance is transformed into digital numbers (DN) for storage and transfer. By transforming the DN values into thermal radiance, followed by conversion of radiance into brightness temperature, it is possible to compute the brightness temperature from Landsat-8 data (Wang et al., 2015). Satellite imagery that includes the first and second study areas were georeferenced to the WGS 84 UTM 33 N coordinate system, while satellite imagery that includes the third study area were georeferenced to the WGS 84 UTM 34 N coordinate system. Finally, for visualization of results, all study areas were georeferenced to the WGS 84 UTM 33 N coordinate system.

3.2. Spectral indices

Interaction with radiation of each specific substrate is described by the spectral signature whose properties are the basis for developing spectral indices. Spectral indices emphasize certain characteristics of land cover, which are formed as a combination of multispectral bands. An index is defined as a synthetic variable having an ordinal scale characterizing the intensity or the extension of overly complex phenomenon to be separated into a manageable number of parameters (Caloz & Collet, 2001).

For the purposes of this research, it is necessary to classify the

Table 1
Landsat-8 satellite imagery used in this research.

Study area	Sensing date	Satellite imagery ID	Path/row
Rijeka	5 August 2013	LC08_L1TP_190029_20130805_20170503_01_T1	190/29
Zagreb	19 July 2015	LC08_L1TP_189028_20150719_20170407_01_T1	189/28
Sarajevo	11 August 2017	LC08_L1TP_187030_20170811_20170824_01_T1	187/30

Table 2
Descriptions of land cover classes.

Class	Description
Water	All forms of water, such as seas, rivers, and lakes
High vegetation	All types of forests and woody vegetation
Low vegetation	Mixtures of cropland, grassland and other forms of undergrowth
Bare land	Empty surfaces, such as soil, rocks, and karst plains
Built-up	Concrete and asphalt surfaces, such as buildings, roads, and airports

Landsat satellite imagery for the five most common land cover classes, namely, water, high vegetation, low vegetation, bare land and built-up (Table 2), based on similar research by Rawat & Kumar, 2015; Natarajan, Latva-Käyrä, Zyadin, & Pelkonen, 2016; Yu, Zhou, Qian, & Yan, 2016; Baskan, Dengiz, & Demirag, 2017; Li, Wang, Zhong, Zhang, & Liu, 2017.

Spectral indices were used to emphasize areas where certain land cover classes dominate. Currently, in order to make spectral indices more accurate, scientists test existing spectral indices, create new indices, and test their accuracy. For the purpose of this research, i.e., to emphasize the water, high vegetation, low vegetation, bare land, and built-up classes, several spectral indices such as the normalized difference water index (NDWI) (Gao, 1996), the enhanced vegetation index (EVI2) (Jiang, Huete, Didan, & Miura, 2008), the index-based built-up index (IBI) (Xu, 2008), and the enhanced built-up and bareness index (EBBI) (As-syakur, Adnyana, Arthana, & Nuarsa, 2012) were tested. Empirical spectral indices, including the modified normalized difference water index (MNDWI) (Xu, 2006), the normalized difference vegetation index (NDVI) (Tucker, 1979), the normalized difference bareness index (NDBaI) (Zhao & Chen, 2005) and the normalized difference bare land index (NBLI) (Li, Wang, Zhong, Su, et al., 2017), have proven to be most appropriate for our studies.

The MNDWI, described by Xu (2006), is one of the most widely used water indices for a variety of applications, including surface water mapping, land cover change analyses and ecological research (Davranche, Lefebvre, & Poulin, 2010; Duan & Bastiaanssen, 2013; Feyisa, Meilby, Fensholt, & Proud, 2014; Hui, Xu, Huang, Yu, & Gong, 2008; Poulin, Davranche, & Lefebvre, 2010). The MNDWI can be expressed as follows (Li, Jiang, & Feng, 2014):

$$MNDWI = \frac{\mathrm{Green}-\mathrm{SWIR1}}{\mathrm{Green}+\mathrm{SWIR1}} \tag{1}$$

where Green is a green band, such as Landsat-8 band 3 (0.533–0.590 μm) and SWIR1 is a shortwave infrared band, such as Landsat-8 band 6 (1.566–1.651 μm). Water has positive values for this index and for built-up land, such as soil and vegetation, has negative values (Xu, 2006).

The NDVI is often used as a monitoring tool for vegetation health and dynamics, enabling easy temporal and spatial comparisons (Myneni, Keeling, Tucker, Asrar, & Nemani, 1997). The NDVI is derived from the red and near-infrared reflectance ratio (Myneni, Hall, Sellers, & Marshak, 1995; Running, 1990; Tucker, 1979):

$$\mathrm{NDVI} = \frac{\mathrm{NIR} - \mathrm{Red}}{\mathrm{NIR} + \mathrm{Red}} \tag{2}$$

where NIR is a near-infrared band such as Landsat-8 band 5 (0.851–0.879 μm) and Red is a red band such as Landsat-8 band 4 (0.636–0.673 μm). NDVI values thus range from −1 to +1, where negative values correspond to the absence of vegetation (Myneni et al., 1995).

According to Zhao and Chen (2005), NDBaI enables differentiation of primary bare lands, secondary bare lands and fallow lands. This index is based on significant differences in the spectral signature in the near-infrared between bare soil and the background. NDBaI is calculated as follows (Zhao & Chen, 2005):

$$NDBaI = \frac{\mathrm{SWIR1} - \mathrm{TIR}}{\mathrm{SWIR1} + \mathrm{TIR}} \tag{3}$$

where SWIR1 is a short-wavelength infrared band such as Landsat-8 band 6 (1.566–1.651 μm) and TIR is thermal infrared band such as Landsat-8 band 10 (10.600–11.190 μm). By selecting an appropriate threshold, different types of bare land can be detected (Zhao & Chen, 2005).

NBLI (Li, Wang, Zhong, Su, et al., 2017) separates the bare land from the other land cover classes. In particular, the difference between bare land and built-up areas becomes great enough to be easily separated. NBLI is defined as follows (Li, Wang, Zhong, Su, et al., 2017):

$$NBLI = \frac{\mathrm{Red} - \mathrm{TIR}}{\mathrm{Red} + \mathrm{TIR}}, \tag{4}$$

where Red is Landsat-8 band 4 (0.636–0.673 μm) and TIR is Landsat-8 band 10 (10.600–11.190 μm). A particular problem is that water bodies containing large amounts of suspended soil may have values similar to those of bare land. To avoid this problem, water must be removed in advance (Li, Wang, Zhong, Su, et al., 2017; Li, Wang, Zhong, Zhang, & Liu, 2017).

For all three study areas, in order to emphasize the areas dominated by a particular land cover, the following four new rasters were created: the modified normalized difference water index (MNDWI), the normalized difference vegetation index (NDVI), the normalized difference bareness index (NDBaI) and the normalized difference bare land index (NBLI) by use of the SAGA GIS software (version 6.2.0).

3.3. Using k-means unsupervised classification

The primary problem with automatic extraction of individual land cover areas from a single index raster is determination of the threshold value. Index value ranges for different land cover types fall in certain ranges and are specific to each satellite imagery scene (Lee, Chen, Wang, & Zhao, 2011). Determining thresholds for separation of individual land cover types in each satellite image is a difficult and lengthy process (Xian, Homer, & Fry, 2009; Zuur, Ieno, & Smith, 2007). According to Li, Wang, Zhong, Su, et al. (2017), k-means unsupervised classification can be used to extract a specific land cover. The k-means algorithm is a popular and well known algorithm for partitioning data into k clusters. It is assumed that the number of clusters, k, is known in advance (Gllavata, Ewerth, & Freisleben, 2004). Using k-means unsupervised classification, water, vegetation, bare land and built-up classes are extracted from MNDWI, NDVI, NDBaI and NBLI rasters, respectively. The novel ALCC method is developed by first distinguishing classes that show higher contrast to the rest of the satellite scene imagery. Accordingly, the water class is first extracted from the MNDWI raster; then, the high and low vegetation classes are extracted from the NDVI raster, and finally, the bare land class is extracted from

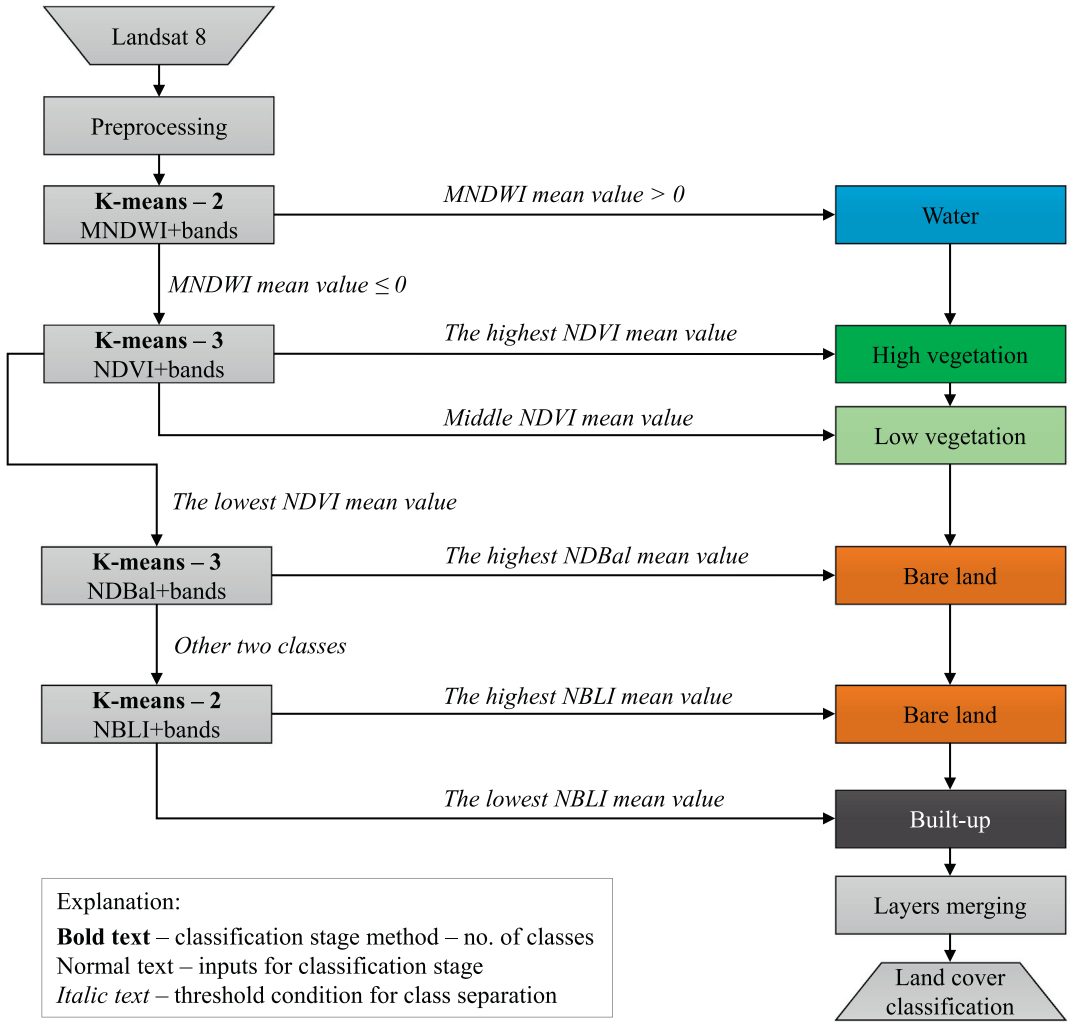

Fig. 2. Workflow of the ALCC method.

the NDBaI and NBLI rasters. Fig. 2 shows the workflow for the ALCC method.

First, the water is extracted from the MNDWI raster, using k-means unsupervised classification, which splits the raster into two classes. The class with the higher mean value represents water. The MNDWI raster is divided into two new rasters, namely, *MNDWI_water* and *MNDWI_land,* containing other land cover types (high and low vegetation, bare land, built-up). The water class is removed from the NDVI raster. This raster is then divided into three classes by k-means unsupervised classification. The highest mean value class represents the high vegetation class, the middle mean value class represents the low vegetation class, and the lowest mean value class represents the other land cover types (bare land and built-up). Three new rasters, namely, *NDVI_lowveg*, *NDVI_highveg*, and *NDVI_other*, are created. From the NDBaI raster, water, low vegetation and high vegetation are removed. According to Li, Wang, Zhong, Su, et al. (2017), it is possible to extract only bare land from the NDBaI raster but, due to the small differences between the bare land and built-up values and the specifics of karst relief (particularly noticeable in the Rijeka study area) the raster NDBaI is divided into three classes. The class with the highest mean value represents bare land, while the remaining two classes represent a built-up class and a bare land class whose value is close to the value for the built-up class. Two new rasters, *NDBaI_bareland* and *NDBaI_others,* are created. Finally, the NBLI which contains only the remaining bare land class and built-up class is divided into two classes using k-means unsupervised classification where a higher mean value represents bare land and the second class represents the built-up class. The classified scene is then generated by merging all rasters with extracted certain land cover type in one raster. Based on the above-described workflow (Fig. 2) and according to the mean value of the classified indices, the automatic algorithm extracts the final land cover classes.

For scientific curiosity, another variant of the ALCC method was explored. The order of flow of the method is the same, but a k-means unsupervised classification is performed over the rasters of individual indices and another six Landsat-8 30 m spatial resolution bands.

The algorithms for both variants of the method were created in SAGA GIS, using the toolchain and are fully automated. Since SAGA GIS is open-source software and is publicly available, implementation of this method for future research is very accessible and straightforward.

3.4. Accuracy assessment

For comparison of the results of the novel ALCC method presented in this study, all three study areas were classified using two commonly used supervised classification methods: The Maximum Likelihood Classification (MLC) and the Random Forests classification (RF). MLC is one of the most widely used image processing routines in remote sensing (Erbek, Özkan, & Taberner, 2004; Foody, Campbell, Trodd, & Wood, 1992; Rawat & Kumar, 2015). Most current maximum likelihood classifiers calculate relative class membership "likelihoods" incorporating all training sets for each pixel in an image. The resultant most likely class identity is then assigned to the output image and the intermediate computational results are discarded (Bolstad & Lillesand, 1991). The RF method is an ensemble learning algorithm that produces multiple decision trees based on a random subset of the training samples and the locations of splits within each decision tree are based on a random subset of the input predictors (Belgiu & Drăguţ, 2016). Satellite imagery scenes were divided into five classes (described in Table 2) by MLC and RF supervised LCC methods. MLC and RF were performed on the same training samples, which were collected by visual inspection of RGB composite rasters from Landsat-8 at 30 m spatial resolution and from Sentinel-2 at 10 m spatial resolution while using the closest acquisition time of Sentinel-2 imagery to that of the Landsat-8 imagery used.

The classification accuracy assessment was undertaken based on the work of Gašparović and Jogun (2018). Reference samples for land cover classification accuracy assessment were determined independently from the classification results using Sentinel-2 and Landsat-8 satellite imagery and without overlap with training samples. For the Rijeka study area, 824 reference samples were collected, i.e., 1.06% of the total area. A total of 553 reference samples were collected for the Zagreb study area, i.e., 1.63% of the total area. For the Sarajevo study area, 457 reference samples were collected, i.e., 1.46% of the total area. Following Pontius and Millones (2011), the figure of merit (F), overall agreement (A), omission (o) and commission (c) were used for quantitative accuracy assessment.

4. Results

As mentioned before, the first step after preprocessing was to create rasters of individual spectral indices. Fig. 3 shows MNDWI, NDVI, NDBaI and NBLI rasters.

From Fig. 3, we see that water in the MNDWI raster has the highest value and is very well separated from the other land cover types. It is also noticeable that vegetation is prominent in the NDVI raster. The next two rasters, NDBaI and NBLI, show that bare land is clearly defined.

A classified scene with five land cover classes was obtained by automatic extraction of certain classes from the spectral indices rasters (MNDWI, NDVI, NDBaI and NBLI) using k-means unsupervised classification. The two methods of automatic classification of the raster scene differ in which input rasters for k-means unsupervised classification. In the first method, k-means is performed only on the spectral indices rasters, while in the second method k-means is performed on the spectral indices rasters and the six Landsat-8 30 m spatial resolution bands (Fig. 4).

To achieve improved visual inspection, the Rijeka study area is divided into two example subsets. By visual inspection of the classification results and a comparison with the RGB composite, we observe that the method using six bands and spectral indices rasters for the unsupervised classification produced a better result. For example subset no. 1, it is evident that the method using spectral indices and six bands better separates bare land from the built-up class, while the method using only the spectral indices rasters overstates the extent of the built-up class. The difference between these two methods becomes much greater for example subset no. 2. The karst relief contained in the bare land class is better classified by the method that uses six bands and spectral indices rasters. Both methods exhibit similar differentiation of the water, low vegetation and high vegetation classes. To confirm these statements objectively, an accuracy assessment of these two methods was made (Table 3).

Table 3 confirms our observations based on the visual inspection. The largest difference between the two variants of the novel method is for the classification of the built-up class, where the classification accuracy for the variant of our method which uses spectral indices and six bands is better. The results obtained indicate that classification accuracy for all classes is much better when utilizing the version of our method which incorporates spectral indices and six bands, with the exception of classification accuracy for the low vegetation class. The difference between the two variants of the method for classification accuracy of the low vegetation class is small. Based on the previous quantitative and visual assessment, the variant of the novel method using spectral indices and six bands proves to be superior, and this is the variant of our method that will be used in further research.

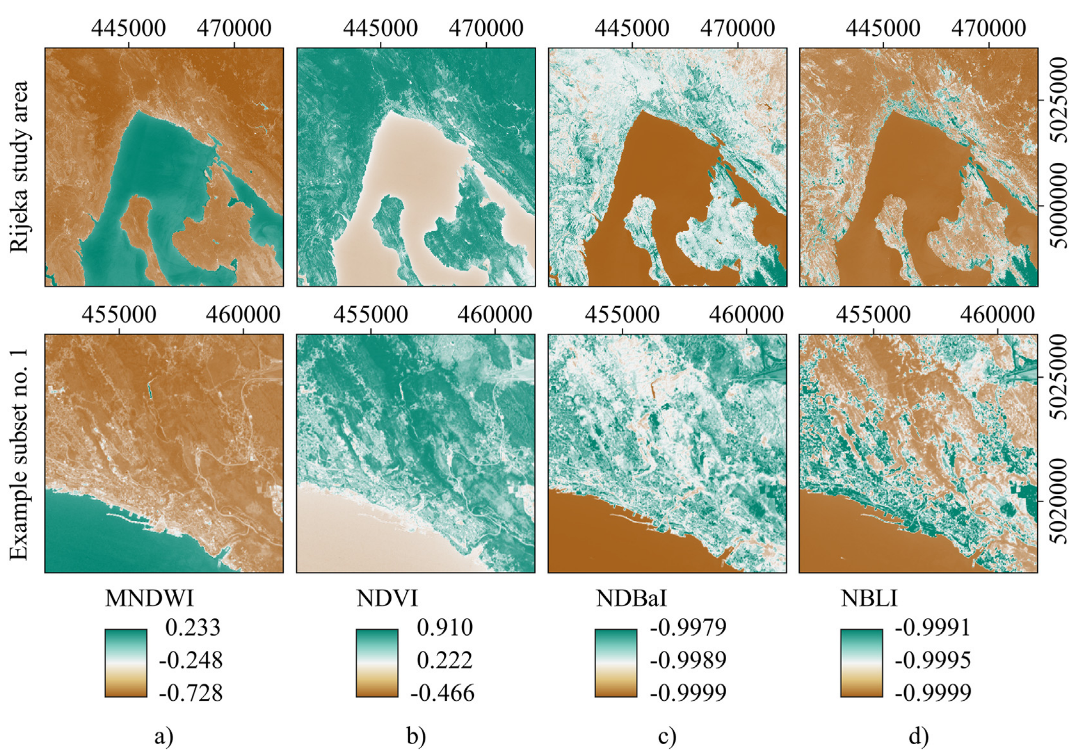

Fig. 3. a) MNDWI; b) NDVI; c) NDBaI; d) NBLI rasters in the Rijeka study area.

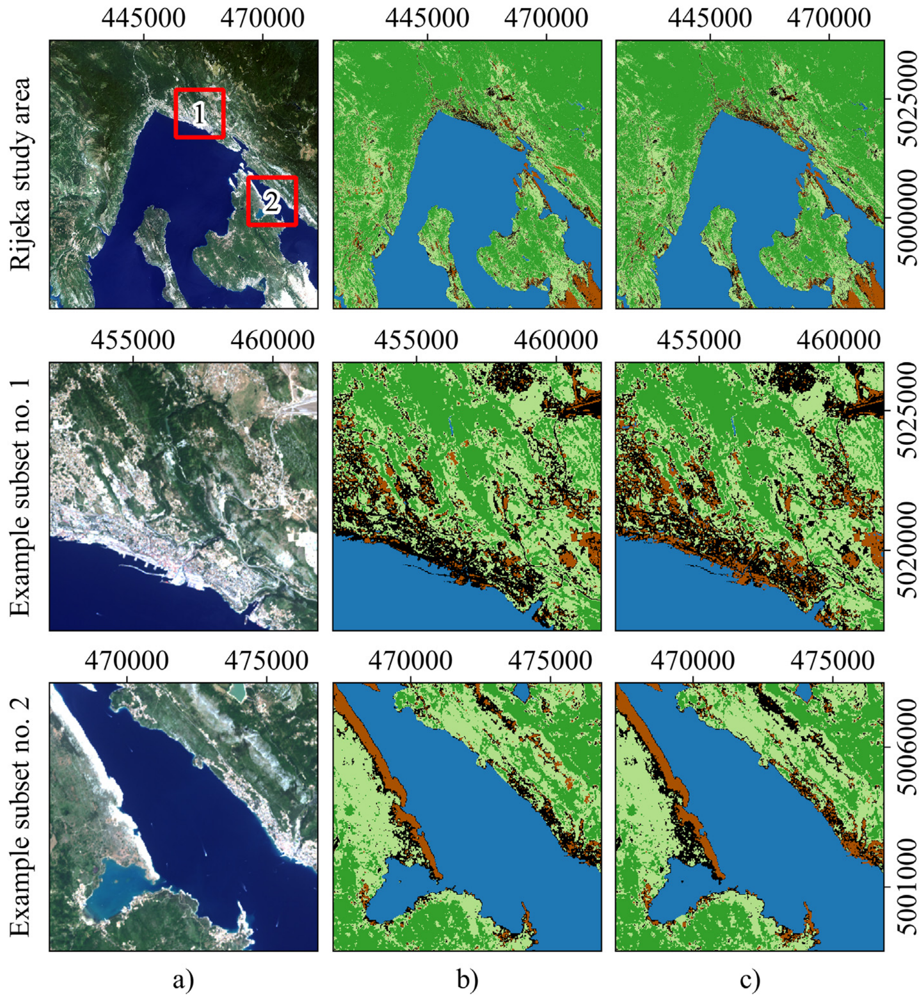

Fig. 4. The results of automatic classification in the Rijeka study area: a) RGB composite; b) results of the method in which k-means is performed on rasters of spectral indices with six Landsat-8 30 m spatial resolution bands; c) results of the method in which k-means is performed based on rasters of spectral indices.

To demonstrate the applicability of the ALCC method, two more scenes, the Zagreb study area and the Sarajevo study area, were classified. The supervised LCC based RF and MLC methods were applied to all three study areas. The average time required to perform ALCC, MLC and RF classification methods was 660 s, 120 s and 30 s, respectively. Additionally, the average time required to perform RF and MLC classifications should be added to the time required for creating representative training samples, which is approximately 1500 s. Based on the previously mentioned duration for all steps needed for land cover classification procedures, it is obvious that our ALCC method is approximately, when comparing relative times, three times faster than normal supervised (MLC or RF) methods (included time for training sample collection). To better compare the results of the proposed automatic classification method with the usual methods of supervised classification, Fig. 5 was constructed.

First, Fig. 5 shows wide applications of the ALCC method, which can be successfully implemented for different types of satellite imagery scenes. Second, the high vegetation and low vegetation classes were classified quite similarly using all three methods. Furthermore, for the example subset no. 3, the ALCC method classified clouds as water, while the other two methods classified clouds as bare land. Additionally, only the ALCC method, e.g., subset no. 4, classified small rivers as water. Visual inspection has determined that RF classifies the built-up class most accurately while MLC overestimates the built-up class and, conversely, the proposed method underestimates the built-up class. The ALCC method overestimates the bare land class, whereas the MLC method underestimates this class. To confirm the visual analysis, the results of accuracy assessment for all classification methods are shown in Table 4.

The classification accuracy for water was similar for all classifications, except in the Sarajevo study area, where the ALCC method gave the best results. The ALCC method proved to be the best method for

Table 3
Classification accuracies for two variants (spectral indices, spectral indices and six bands) of the novel ALCC method for the Rijeka study area.

ALCC method variants	Water			High vegetation			Low vegetation			Built-up			Bare land			A
	F	o	c	F	o	c	F	o	c	F	o	c	F	o	c	
Spectral indices	99.1	< 0.1	0.4	89.3	1.6	0.8	67.6	2.2	2.4	40.1	3.9	4.8	58.8	3.8	3.3	88.4
Spectral indices and six bands	99.8	< 0.1	0.1	90.3	1.3	0.8	66.8	2.1	2.8	49.2	2.8	4.2	63.8	3.7	2.1	90.0

F: figure of merit (%); o: omission (%); c: commission (%); A: overall agreement (%).

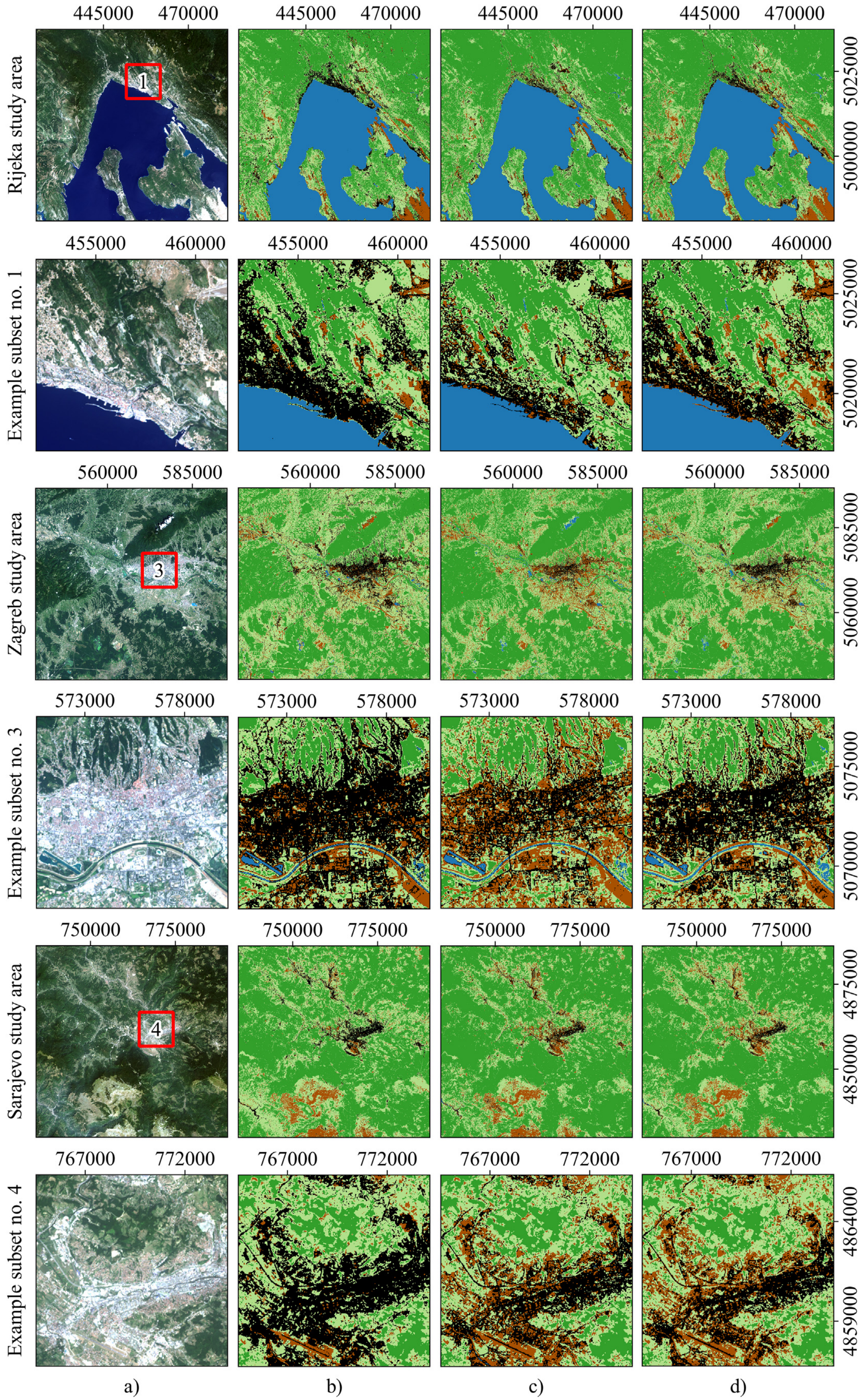

Fig. 5. The results of applied classification methods for the different study areas: a) RGB composite; b) MLC; c) ALCC; d) RF.

Table 4
Classification accuracies for three classification methods for the three study areas.

Study area	Classification method	Water			High vegetation			Low vegetation			Built-up			Bare land			A
		F	o	c	F	o	c	F	o	c	F	o	c	F	o	c	
Rijeka	MLC	99.5	0.2	< 0.1	85.3	2.8	0.4	55.8	3.2	3.7	51.6	1.4	6.3	62.8	4.3	1.5	88.1
	ALCC	99.8	< 0.1	0.1	90.3	1.3	0.8	66.8	2.1	2.8	49.2	2.8	4.2	63.8	3.7	2.1	90.0
	RF	99.6	< 0.1	0.2	92.4	1.3	0.4	66.4	2.9	1.7	62.6	2.4	1.9	67.8	1.7	4.2	91.7
Zagreb	MLC	94.3	0.3	0.0	91.5	3.3	1.6	69.7	3.0	4.0	65.5	2.5	2.0	53.2	1.9	3.5	88.9
	ALCC	97.9	0.1	< 0.1	93.2	0.4	3.7	69.7	5.0	1.3	59.6	4.1	0.6	55.3	0.9	4.9	89.5
	RF	98.2	0.1	< 0.1	93.3	0.6	3.4	69.7	4.8	1.5	69.8	2.3	1.4	55.8	1.8	3.2	90.4
Sarajevo	MLC	0.0	2.1	0.0	91.4	5.0	0.2	59.7	1.1	6.9	60.5	0.3	5.3	66.2	4.8	0.9	86.7
	ALCC	98.8	< 0.1	< 0.1	94.0	1.6	2.1	61.7	2.6	3.9	66.9	1.5	2.1	64.4	4.5	1.9	89.9
	RF	81.5	0.1	0.3	93.7	1.9	2.0	60.5	2.3	4.8	75.3	1.1	1.5	67.3	4.4	1.2	90.2

F: figure of merit (%); o: omission (%); c: commission (%); A: overall agreement (%).

extracting the water class in the Rijeka study area. The figure of merit for high vegetation was over 90%, except when the MLC classification method was used in the Rijeka study area. The classification accuracy for the high vegetation class was the best for the RF method, except in the Sarajevo study area, where the ALCC method yielded the best results. The classification accuracy for low vegetation was low for all classifications on all study areas, but the ALCC method gave a slightly better result for all study areas. The classification accuracy for the built-up class was lowest for the Rijeka study area for all classification methods. In the Rijeka study area, the ALCC method yielded the least accurate results while the largest difference between omission and commission was for the MLC method. The worst accuracy for the bare land class was in the Zagreb study area when using the MLC classification method, while the RF method provided the best results for all study areas. Finally, it is important to note that the overall agreement of the ALCC method always fell between the overall agreements of the MLC and RF methods and was much closer to the RF. According to this accuracy assessment, the RF classification provided a better overall classification while ALCC better classifies the water and low vegetation classes. As expected, MLC has lower accuracy than RF and ALCC.

5. Discussion

Global and regional assessments of land cover and of land use status and changes are of fundamental importance for climate and environmental change studies (Foley et al., 2005; Matthews, Weaver, Meissner, Gillett, & Eby, 2004; Turner, Lambin, & Reenberg, 2007). Through classification, we can obtain insights into the state of the land surface. Remote sensing classification is a complex process and requires consideration of many factors. The major steps for image classification may include determination of a suitable classification system, selection of training samples, image preprocessing, feature extraction, selection of suitable classification approaches, post-classification processing, and accuracy assessment (Lu & Weng, 2007). Although there are many classification methods in use, it cannot be stated with confidence which is the most complete. Application of the various methods depends on the input data and on the use of the final classification results. For the requirements of large area analysis, all known methods require much time and experience in implementation, analysis and interpretation. This research contributes to classification methods by demonstrating the importance of our new automatic method. Although Baraldi et al. (2005) and Baraldi et al. (2006) described the fundamentals of the automatic classification method, this research has modified these existing methods and approaches and has also compared the accuracy of known and novel ALCC classification methods.

Consistent with recent research advocating the importance of using spectral indices (Baraldi et al., 2006; Deilami, Kamruzzaman, & Hayes, 2016; Lee et al., 2011; Li et al., 2014; Xu, 2007; Yang, Weisberg, & Bristow, 2012), our findings indicate that using MNDWI, NDVI, NDBaI and NBLI spectral indices rasters can highlight certain land cover types, being the basis for their extraction. Furthermore, the workflow used in this research is quite simple and provides a method that is easy to implement and for which execution time is short. Additionally, our workflow results in no unclassified pixels, which occurs for some classification methods. To our knowledge, this is the first research that provides an automatic classification method based on spectral indices and six Landsat-8 bands. By objective and subjective analysis, this method, using the spectral indices and six band rasters, has been demonstrated to be superior. The results of this study show that the ALCC method is applicable to landscapes containing various land cover types and whose final classification is similar to the final classification of already well-known and applied classification methods (MLC and RF). Furthermore, we compared the accuracy assessment of the three classification methods and found that their accuracy assessment is most similar for the high vegetation class. The best accuracy assessment for the low vegetation class uses an ALCC method, as expected; the k-means methods use statistical indicators for class separation, while supervised classification uses data from the subject to determine training samples. Moreover, the ALCC method distinguishes the water class most accurately, as is demonstrated in the Sarajevo study area. The three methods of classification used in this study have the highest difference in accuracy for classifying the built-up and bare land classes. The ALCC method has been shown as the least accurate for extracting the built-up class, which is quite logical and justified. First, the proposed method is based on spectral indices, where calculation of spectral indices emphasizing built-up areas includes a Landsat-8 thermal band with an original spectral resolution of 100 m. Second, mixed pixels have been recognized as a problem impacting effective use of remote sensing data for urban land use/land cover classification (Cracknell, 1998; Fisher, 1997). Due to the use of a thermal band related to the urban heat island (UHI) effect, separation of the built-up and bare land classes is not straightforward. The UHI effect is a phenomenon in which urban areas experience higher temperatures compared to surrounding non-urban areas (Deilami et al., 2016). Moreover, the nature of the MLC classification method is such that it overestimates the built-up class. Hence, its accuracy assessment of the built-up class is higher. On the other hand, by comparing the MLC and ALCC methods, the ALCC method classifies the bare land class with higher accuracy. To improve the performance of the ALCC method in build-up areas, future studies should include pansharpening (Aiazzi, Baronti, & Selva, 2007; Alparone et al., 2007) or fusion with other sensors (Gašparović & Jogun, 2018; Zeng, Huang, Liu, Zhang, & Zou, 2010). By visual inspection as well as statistical indicators, the RF method has shown to be the best method of classification, followed by an ALCC method. RF is efficient for large databases and is relatively robust in the presence of outliers and noise such as the fast classification method (Breiman, 2001; Feng, Liu, & Gong, 2015; Rodriguez-Galiano, Ghimire, Rogan, Chica-Olmo, & Rigol-Sanchez, 2012). When classifying large areas by the RF method, much time is lost for collecting the correct training samples (approximately 1500 s). Although the RF gave slightly better classification results than the proposed ALCC method, our proposed method would be a more cost-effective choice as it is fully automated through use of the toolchain in SAGA GIS and only requires preprocessing of satellite imagery.

One of the limitations of this research and of our novel method is the predetermined number of classes. A small number of classes (only five) are used in this research as this is common practice when developing new approaches and methods (Baskan et al., 2017; Li, Wang, Zhong, Zhang, & Liu, 2017; Natarajan et al., 2016; Rawat & Kumar, 2015; Yu et al., 2016). In future studies, it will be necessary to explore the possibility of defining more classes, such as dividing the low vegetation class into cropland and grassland classes. Additionally, in future work, the method should be applied to areas that are shaded and covered with clouds. The main limitation of this research is that the method is based on a thermal band which does not use all available high-resolution sensors. To apply the automatic method to high-resolution data, future studies should develop spectral indices that extract individual land cover types equally well, but which would not be based on the thermal band.

6. Conclusions

Presently, in a world undergoing rapid changes in the environment, it is extremely important to detect changes on the terrestrial surface. Remote sensing plays a major role in detecting changes in large areas of the surface of the earth. To detect such changes, it is necessary to classify satellite imagery scenes. All known and applied classification methods are limited by the time spent in preprocessing or postprocessing.

With a goal of improving existing classification methods, we have created a novel automatic classification method based on the use of spectral indices rasters and unsupervised classification k-means. In terms of accuracy assessment, the version of the ALCC which used both spectral indices and six Landsat 8 OLI bands as input to the k-means clustering was found to be superior to the version that used spectral indices alone. This novel method is automatic, cost-effective, practical, easy to use in other study areas, does not require a large number of computer operations and, most importantly, is of high accuracy.

The subject and purpose of this research, as well as the novel method based on open-source software, are of great importance for global applications. Global application of the ALCC method, when using different sensors and applied to different study areas, can remove current limitations of our classification methods and provide improvements.

Conflict of interest

This manuscript has not been published and is not under consideration for publication elsewhere. Authors have no conflicts of interest to disclose.

Acknowledgements

The authors would like to thank the anonymous reviewers for their valuable comments and suggestions on improving the quality of the paper.

References

Abadi, M., Barham, P., Chen, J., Chen, Z., Davis, A., Jeffrey, D., ... Zheng, X. (2016). Tensorflow: A system for large-scale machine learning. *Proceedings of the 12th USENIX symposium on operating systems design and implementation* (pp. 265–283). Savannah, USA: USENIX Association.

Aiazzi, B., Baronti, S., & Selva, M. (2007). Improving component substitution pan-sharpening through multivariate regression of MS + pan data. *IEEE Transactions on Geoscience and Remote Sensing, 45*, 3230–3239. https://doi.org/10.1109/TGRS.2007.901007.

Alparone, L., Wald, L., Chanussot, J., Thomas, C., Gamba, P., & Bruce, L. M. (2007). Comparison of pansharpening algorithms: Outcome of the 2006 GRS-S data-fusion contest. *IEEE Transactions on Geoscience and Remote Sensing, 45*, 3012–3021. https://doi.org/10.1109/TGRS.2007.904923.

As-syakur, A. R., Adnyana, I. W. S., Arthana, I. W., & Nuarsa, I. W. (2012). Enhanced built-up and bareness index (EBBI) for mapping built-up and bare land in an urban area. *Remote Sensing, 4*, 2957–2970. https://doi.org/10.3390/rs4102957.

Baraldi, A. (2011). Fuzzification of a crisp near-real-time operational automatic spectral-rule-based decision-tree preliminary classifier of multisource multispectral remotely sensed images. *IEEE Transactions on Geoscience and Remote Sensing, 49*, 2113–2134. https://doi.org/10.1109/TGRS.2010.2091137.

Baraldi, A., & Boschetti, L. (2012). Operational automatic remote sensing image understanding systems: Beyond geographic object-based and object-oriented image analysis (GEOBIA/GEOOIA). Part 1: Introduction. *Remote Sensing, 4*, 2694–2735. https://doi.org/10.3390/rs4092694.

Baraldi, A., Bruzzone, L., & Blonda, P. (2005). Quality assessment of classification and cluster maps without ground truth knowledge. *IEEE Transactions on Geoscience and Remote Sensing, 43*, 857–873. https://doi.org/10.1109/TGRS.2004.843074.

Baraldi, A., Puzzolo, V., Blonda, P., Bruzzone, L., & Tarantino, C. (2006). Automatic spectral rule-based preliminary mapping of calibrated Landsat TM and ETM + images. *IEEE Transactions on Geoscience and Remote Sensing, 44*, 2563–2586. https://doi.org/10.1109/TGRS.2006.874140.

Baskan, O., Dengiz, O., & Demirag, İ. T. (2017). The land productivity dynamics trend as a tool for land degradation assessment in a dryland ecosystem. *Environmental Monitoring and Assessment, 189*, 212. https://doi.org/10.1007/s10661-017-5909-3.

Belgiu, M., & Drăguţ, L. (2016). Random forest in remote sensing: A review of applications and future directions. *ISPRS Journal of Photogrammetry and Remote Sensing, 114*, 24–31. https://doi.org/10.1016/J.ISPRSJPRS.2016.01.011.

Bezdek, J. C. (1980). A convergence theorem for the fuzzy ISODATA clustering algorithms. *IEEE Transactions on Pattern Analysis and Machine Intelligence, PAMI-2*, 1–8. https://doi.org/10.1109/TPAMI.1980.4766964.

Bolstad, P. V., & Lillesand, T. M. (1991). Rapid maximum likelihood classification. *Photogrammetric Engineering and Remote Sensing, 57*, 67–74.

Breiman, L. (2001). Random forests. *Machine Learning, 45*, 5–32. https://doi.org/10.1023/A:1010933404324.

Caloz, R., & Collet, C. (2001). *Précis de télédétection-Volume 3: Traitements numériques d'images de télédétection.* Quebec: Presses de l'Université du Québec.

Chavez, P. S. (1989). Radiometric calibration of Landsat thematic mapper multispectral images. *Photogrammetric Engineering and Remote Sensing, 55*, 1285–1294.

Clark, M. L., Aide, T. M., & Riner, G. (2012). Land change for all municipalities in Latin America and the Caribbean assessed from 250-m MODIS imagery (2001 – 2010). *Remote Sensing of Environment, 126*, 84–103. https://doi.org/10.1016/J.RSE.2012.08.013.

Cracknell, A. P. (1998). Review article synergy in remote sensing-what's in a pixel? *International Journal of Remote Sensing, 19*, 2025–2047. https://doi.org/10.1080/014311698214848.

Davranche, A., Lefebvre, G., & Poulin, B. (2010). Wetland monitoring using classification trees and SPOT-5 seasonal time series. *Remote Sensing of Environment, 114*, 552–562. https://doi.org/10.1016/J.RSE.2009.10.009.

Deilami, K., Kamruzzaman, M., & Hayes, J. F. (2016). Correlation or causality between land cover patterns and the urban heat island effect? Evidence from Brisbane, Australia. *Remote Sensing, 8*, 716. https://doi.org/10.3390/rs8090716.

Duan, Z., & Bastiaanssen, W. G. M. (2013). Estimating water volume variations in lakes and reservoirs from four operational satellite altimetry databases and satellite imagery data. *Remote Sensing of Environment, 134*, 403–416. https://doi.org/10.1016/J.RSE.2013.03.010.

Erbek, F. S., Özkan, C., & Taberner, M. (2004). Comparison of maximum likelihood classification method with supervised artificial neural network algorithms for land use activities. *International Journal of Remote Sensing, 25*, 1733–1748. https://doi.org/10.1080/0143116031000150077.

Estoque, R. C., & Murayama, Y. (2015). Classification and change detection of built-up lands from Landsat-7 ETM + and Landsat-8 OLI/TIRS imageries: A comparative assessment of various spectral indices. *Ecological Indicators, 56*, 205–217. https://doi.org/10.1016/J.ECOLIND.2015.03.037.

Feng, Q., Liu, J., & Gong, J. (2015). UAV remote sensing for urban vegetation mapping using random forest and texture analysis. *Remote Sensing, 7*, 1074–1094. https://doi.org/10.3390/rs70101074.

Feyisa, G. L., Meilby, H., Fensholt, R., & Proud, S. R. (2014). Automated water extraction index: A new technique for surface water mapping using Landsat imagery. *Remote Sensing of Environment, 140*, 23–35. https://doi.org/10.1016/J.RSE.2013.08.029.

Fisher, P. (1997). The pixel: A snare and a delusion. *International Journal of Remote Sensing, 18*, 679–685. https://doi.org/10.1080/014311697219015.

Foley, J. A., Defries, R., Asner, G. P., Barford, C., Bonan, G., Carpenter, S. R., ... Snyder, P. K. (2005). Global consequences of land use. *Science, 309*, 570–574. https://doi.org/10.1126/science.1111772.

Foody, G. M. (2002). Status of land cover classification accuracy assessment. *Remote Sensing of Environment, 80*, 185–201. https://doi.org/10.1016/S0034-4257(01)00295-4.

Foody, G. M., Campbell, N. A., Trodd, N. M., & Wood, T. F. (1992). Derivation and applications of probabilistic measures of class membership from the maximum-likelihood classification. *Photogrammetric Engineering and Remote Sensing, 58*, 1335–1341.

Gao, B. (1996). NDWI–A normalized difference water index for remote sensing of vegetation liquid water from space. *Remote Sensing of Environment, 58*, 257–266. https://doi.org/10.1016/S0034-4257(96)00067-3.

Gašparović, M., & Jogun, T. (2018). The effect of fusing Sentinel-2 bands on land-cover classification. *International Journal of Remote Sensing, 39*, 822–841. https://doi.org/10.1080/01431161.2017.1392640.

Gislason, P. O., Benediktsson, J. A., & Sveinsson, J. R. (2006). Random forests for land

cover classification. *Pattern Recognition Letters, 27*, 294–300. https://doi.org/10.1016/J.PATREC.2005.08.011.
Gllavata, J., Ewerth, R., & Freisleben, B. (2004). Text detection in images based on unsupervised classification of high-frequency wavelet coefficients. *Proceedings of the 17th international conference on pattern recognition, 2004. ICPR 2004. Vol. 1. Proceedings of the 17th international conference on pattern recognition, 2004. ICPR 2004* (pp. 425–428). Cambridge, UK: IEEE. https://doi.org/10.1109/ICPR.2004.1334146.
Hartigan, J. A., & Wong, M. A. (1979). Algorithm AS 136: A K-means clustering algorithm. *Applied Statistics, 28*, 100. https://doi.org/10.2307/2346830.
Hermosilla, T., Wulder, M. A., White, J. C., Coops, N. C., & Hobart, G. W. (2015). An integrated Landsat time series protocol for change detection and generation of annual gap-free surface reflectance composites. *Remote Sensing of Environment, 158*, 220–234. https://doi.org/10.1016/J.RSE.2014.11.005.
Huete, A. (1988). A soil-adjusted vegetation index (SAVI). *Remote Sensing of Environment, 25*, 295–309. https://doi.org/10.1016/0034-4257(88)90106-X.
Hui, F., Xu, B., Huang, H., Yu, Q., & Gong, P. (2008). Modelling spatial-temporal change of Poyang Lake using multitemporal Landsat imagery. *International Journal of Remote Sensing, 29*, 5767–5784. https://doi.org/10.1080/01431160802060912.
Jiang, Z., Huete, A. R., Didan, K., & Miura, T. (2008). Development of a two-band enhanced vegetation index without a blue band. *Remote Sensing of Environment, 112*, 3833–3845. https://doi.org/10.1016/J.RSE.2008.06.006.
Krizhevsky, A., Sutskever, I., & Hinton, G. E. (2012). ImageNet classification with deep convolutional neural networks. *Advances in Neural Information Processing Systems, 25*, 1097–1105.
LeCun, Y., Bengio, Y., & Hinton, G. (2015). Deep learning. *Nature, 521*, 436–444. https://doi.org/10.1038/nature14539.
Lee, L., Chen, L., Wang, X., & Zhao, J. (2011). Use of Landsat TM/ETM+ data to analyze urban heat island and its relationship with land use/cover change. *In: 2011 international conference on remote sensing, environment and transportation engineering. IEEE, Nanjing, China* (pp. 922–927). . https://doi.org/10.1109/RSETE.2011.5964429.
Li, H., Wang, C., Zhong, C., Su, A., Xiong, C., Wang, J., & Liu, J. (2017). Mapping urban bare land automatically from Landsat imagery with a simple index. *Remote Sensing, 9*, 249. https://doi.org/10.3390/rs9030249.
Li, H., Wang, C., Zhong, C., Zhang, Z., & Liu, Q. (2017). Mapping typical urban LULC from Landsat imagery without training samples or self-defined parameters. *Remote Sensing, 9*, 700. https://doi.org/10.3390/rs9070700.
Li, P., Jiang, L., & Feng, Z. (2014). Cross-comparison of vegetation indices derived from Landsat-7 enhanced thematic mapper plus (ETM+) and Landsat-8 operational land imager (OLI) sensors. *Remote Sensing, 6*, 310–329. https://doi.org/10.3390/rs6010310.
Lu, D., & Weng, Q. (2007). A survey of image classification methods and techniques for improving classification performance. *International Journal of Remote Sensing, 28*, 823–870. https://doi.org/10.1080/01431160600746456.
Mather, P., & Tso, B. (2016). *Classification methods for remotely sensed data.* Boca Raton: CRC Press.
Matthews, H. D., Weaver, A. J., Meissner, K. J., Gillett, N. P., & Eby, M. (2004). Natural and anthropogenic climate change: Incorporating historical land cover change, vegetation dynamics and the global carbon cycle. *Climate Dynamics, 22*, 461–479. https://doi.org/10.1007/s00382-004-0392-2.
Myneni, R. B., Hall, F. G., Sellers, P. J., & Marshak, A. L. (1995). The interpretation of spectral vegetation indexes. *IEEE Transactions on Geoscience and Remote Sensing, 33*, 481–486.
Myneni, R. B., Keeling, C. D., Tucker, C. J., Asrar, G., & Nemani, R. R. (1997). Increased plant growth in the northern high latitudes from 1981 to 1991. *Nature, 386*, 698–702. https://doi.org/10.1038/386698a0.
Nasrabadi, N. M. (2007). Pattern recognition and machine learning. *Journal of Electronic Imaging, 16*, 049901. https://doi.org/10.1117/1.2819119.
Natarajan, K., Latva-Käyrä, P., Zyadin, A., & Pelkonen, P. (2016). New methodological approach for biomass resource assessment in India using GIS application and land use/land cover (LULC) maps. *Renewable and Sustainable Energy Reviews, 63*, 256–268. https://doi.org/10.1016/J.RSER.2016.05.070.
Otukei, J. R., & Blaschke, T. (2010). Land cover change assessment using decision trees, support vector machines and maximum likelihood classification algorithms. *International Journal of Applied Earth Observation and Geoinformation, 12*, S27–S31. https://doi.org/10.1016/J.JAG.2009.11.002.
Pal, M., & Mather, P. M. (2003). An assessment of the effectiveness of decision tree methods for land cover classification. *Remote Sensing of Environment, 86*, 554–565. https://doi.org/10.1016/S0034-4257(03)00132-9.
Pontius, R. G., & Millones, M. (2011). Death to kappa: Birth of quantity disagreement and allocation disagreement for accuracy assessment. *International Journal of Remote Sensing, 32*, 4407–4429. https://doi.org/10.1080/01431161.2011.552923.
Poulin, B., Davranche, A., & Lefebvre, G. (2010). Ecological assessment of Phragmites australis wetlands using multi-season SPOT-5 scenes. *Remote Sensing of Environment, 114*, 1602–1609. https://doi.org/10.1016/J.RSE.2010.02.014.
Rawat, J. S., & Kumar, M. (2015). Monitoring land use/cover change using remote sensing and GIS techniques: A case study of Hawalbagh block, district Almora, Uttarakhand, India. *Egyptian Journal of Remote Sensing and Space Science, 18*, 77–84. https://doi.org/10.1016/J.EJRS.2015.02.002.
Rodriguez-Galiano, V. F., Ghimire, B., Rogan, J., Chica-Olmo, M., & Rigol-Sanchez, J. P. (2012). An assessment of the effectiveness of a random forest classifier for land-cover classification. *ISPRS Journal of Photogrammetry and Remote Sensing, 67*, 93–104. https://doi.org/10.1016/J.ISPRSJPRS.2011.11.002.
Roy, D. P., Wulder, M. A., Loveland, T. R., Woodcock, C. E., Allen, R. G., Anderson, M. C., ... Zhu, Z. (2014). Landsat-8: Science and product vision for terrestrial global change research. *Remote Sensing of Environment, 145*, 154–172. https://doi.org/10.1016/J.RSE.2014.02.001.
Running, S. W. (1990). Estimating terrestrial primary productivity by combining remote sensing and ecosystem simulation. In R. J. Hobbs, & H. A. Mooney (Vol. Eds.), *Remote sensing of biosphere functioning. Vol. 79. Remote sensing of biosphere functioning* (pp. 65–86). New York: Springer. https://doi.org/10.1007/978-1-4612-3302-2_4 Ecological Studies (Analysis and Synthesis).
Song, C., Woodcock, C. E., Seto, K. C., Lenney, M. P., & Macomber, S. A. (2001). Classification and change detection using Landsat TM data: When and how to correct atmospheric effects? *Remote Sensing of Environment, 75*, 230–244. https://doi.org/10.1016/S0034-4257(00)00169-3.
Suykens, J. A. K., & Vandewalle, J. (1999). Least squares support vector machine classifiers. *Neural Processing Letters, 9*, 293–300. https://doi.org/10.1023/A:1018628609742.
Tucker, C. J. (1979). Red and photographic infrared linear combinations for monitoring vegetation. *Remote Sensing of Environment, 8*, 127–150. https://doi.org/10.1016/0034-4257(79)90013-0.
Turner, B. L., Lambin, E. F., & Reenberg, A. (2007). The emergence of land change science for global environmental change and sustainability. *Proceedings of the National academy of Sciences of the United States of America, 104*, 20666–20671. https://doi.org/10.1073/pnas.0704119104.
Wang, F., Qin, Z., Song, C., Tu, L., Karnieli, A., & Zhao, S. (2015). An improved mono-window algorithm for land surface temperature retrieval from Landsat 8 thermal infrared sensor data. *Remote Sensing, 7*, 4268–4289. https://doi.org/10.3390/rs70404268.
Xian, G., & Homer, C. (2010). Updating the 2001 national land cover database impervious surface products to 2006 using Landsat imagery change detection methods. *Remote Sensing of Environment, 114*, 1676–1686. https://doi.org/10.1016/J.RSE.2010.02.018.
Xian, G., Homer, C., & Fry, J. (2009). Updating the 2001 national land cover database land cover classification to 2006 by using Landsat imagery change detection methods. *Remote Sensing of Environment, 113*, 1133–1147. https://doi.org/10.1016/J.RSE.2009.02.004.
Xu, H. (2006). Modification of normalised difference water index (NDWI) to enhance open water features in remotely sensed imagery. *International Journal of Remote Sensing, 27*, 3025–3033. https://doi.org/10.1080/01431160600589179.
Xu, H. (2007). Extraction of urban built-up land features from Landsat imagery using a thematicoriented index combination technique. *Photogrammetric Engineering and Remote Sensing, 73*, 1381–1391. https://doi.org/10.14358/PERS.73.12.1381.
Xu, H. (2008). A new index for delineating built-up land features in satellite imagery. *International Journal of Remote Sensing, 29*, 4269–4276. https://doi.org/10.1080/01431160802039957.
Yang, J., Weisberg, P. J., & Bristow, N. A. (2012). Landsat remote sensing approaches for monitoring long-term tree cover dynamics in semi-arid woodlands: Comparison of vegetation indices and spectral mixture analysis. *Remote Sensing of Environment, 119*, 62–71. https://doi.org/10.1016/J.RSE.2011.12.004.
Yu, W., Zhou, W., Qian, Y., & Yan, J. (2016). A new approach for land cover classification and change analysis: Integrating backdating and an object-based method. *Remote Sensing of Environment, 177*, 37–47. https://doi.org/10.1016/J.RSE.2016.02.030.
Zeng, Y., Huang, W., Liu, M., Zhang, H., & Zou, B. (2010). Fusion of satellite images in urban area: Assessing the quality of resulting images, in: 2010 18th international conference on geoinformatics. *IEEE*, 1–4. https://doi.org/10.1109/GEOINFORMATICS.2010.5568105.
Zhang, Z., He, G., & Wang, X. (2010). A practical DOS model-based atmospheric correction algorithm. *International Journal of Remote Sensing, 31*, 2837–2852. https://doi.org/10.1080/01431160903124682.
Zhao, H., & Chen, X. (2005). Use of normalized difference bareness index in quickly mapping bare areas from TM/ETM+. *2005 IEEE international geoscience and remote sensing symposium, 2005. IGARSS '05* (pp. 1666–1668). Seoul, South Korea: IEEE. https://doi.org/10.1109/IGARSS.2005.1526319.
Zuur, A. F., Ieno, E. N., & Smith, G. M. (2007). Principal component analysis and redundancy analysis. *Analysing Ecological Data,* 193–224. https://doi.org/10.1007/978-0-387-45972-1_12.